Chaos in mixing vessels

Pavel Hasal[1] and Ivan Fořt[2]

[1] Institute of Chemical Technology, Prague
Department of Chemical Engineering
CZ-166 28 Praha 6, Czech Republic
(e-mail: `Pavel.Hasal@vscht.cz`)
[2] Czech Technical University
Department of Process Engineering
CZ-166 07 Praha 6, Czech Republic
(e-mail: `Ivan.Fort@fs.cvut.cz`)

Abstract. Experimental time series from two geometrically similar mixing vessels are decomposed by Singular Value Decomposition. Low frequency components are identified and extracted and their attractors are reconstructed and the attractor invariants are evaluated in a dependence on operational conditions and fluid properties. Regions with distinct dynamical behaviours are identified within the vessels. The correlation dimension of the attractors is suitable for analysis of transitions between different flow patterns and of different low-frequency flows resulting from these transitions. The maximum Lyapunov exponent can be used to identify regions with dispersive dynamics within the tank.
Keywords: Stirred tank, macro-instability, chaos, attractor, embedding dimension, chaotic invariants.

1 Introduction

Stirred vessels are common in most of process industries where they are used to blend miscible liquids, to disperse a gas into a liquid, to suspend solid particles or to enhance mass and heat transfer, etc. Flow phenomena encountered in the stirred tanks are therefore a subject of numerous theoretical and experimental studies.

The flow of a batch in the stirred tank is highly complex and comprise components vastly differing in their temporal and spatial scales. The spatial scales of particular flows in the vessel extend from sizes comparable to vessel dimensions to microscopic turbulent eddies dissipating the kinetic energy of the liquid. Liquid flow in a stirred vessel can be viewed as a pseudo-stationary, spatially distributed dynamical system with high dimension of its phase space.

A decade or two ago, a particular pseudo-periodic macro-scale flow has been identified in stirred vessels manifesting itself on a spatial scale comparable to the size of the vessel and occurring with characteristic frequencies significantly lower than the impeller frequency. This flow has been named the macro-instability (MI) of the flow pattern. The MI existence has been

confirmed by various experimental methods, see, e.g., Kresta and Wood[1], Brůha *et al.*[2], Montes *et al.*[3], Nikiforaki *et al.*[4], Bittorf and Kresta[5].

The macro-instability of the flow pattern has a strong impact on all mixing processes linked to fluid motions. It, however, also exerts strong forces acting on solid surfaces immersed in a stirred liquid (baffles, cooling and heating coils, etc.) - see, e.g., Kratěna *et al.*[6] and Hasal *et al.*[7]. Detailed knowledge of the formation and time evolution of MI and a quantitative description of it is therefore of great practical importance. Until now the most of experimental efforts has been focused on the frequency of the macro-instability occurrence and to the MI kinetic energy. Our earlier analyses, cf. Hasal *et al.*[8,9], however, have also pointed to the chaotic nature of the macro-instability fluid flow component. It was suggested that MI is probably generated by a low-dimensional dynamical system with deterministically chaotic dynamics. This paper aims to confirm this hypothesis.

Methods of non-linear analysis are applied to the analysis of experimental data from stirred tanks relatively scarcely, probably due to the high spatio-temporal complexity of fluid flow (stochastic turbulent flows) encountered in stirred vessels. Ottino *et al.*[10] described the mixing processes in fluids in terms of a general theory of chaotic processes and suggested links between them and their engineering counterparts. Letellier *et al.*[11] analyzed the velocity field in a standard mixing vessel with a Rushton turbine impeller. They introduced a mathematical procedure, based on an application of the Hilbert transform, enabling the separation of deterministic component from the stochastic component of measured data. An attempt to analyze data from mixing tanks by non-linear methods was performed also by Matsuda *et al.*[12].

2 Experimental

2.1 Stirred Tanks and Experimental Conditions

Two geometrically identical cylindrical flat-bottomed mixing tanks with four radial baffles (see Figure 1) were used in experiments. Two series of experiments have been performed: the axial component of liquid velocity was measured in a close to impeller region in the first series and the tangential component of the force affecting the baffles was studied in the second series.

2.2 Velocity measurement

The axial component of liquid velocity in the stirrer region was measured by the laser Doppler velocimetry (LDV) using the pitched blade impeller pumping liquid towards vessel bottom and located at the off-bottom clearance of $C = 0.35\,T$. Water and two aqueous glycerol solutions were used as working
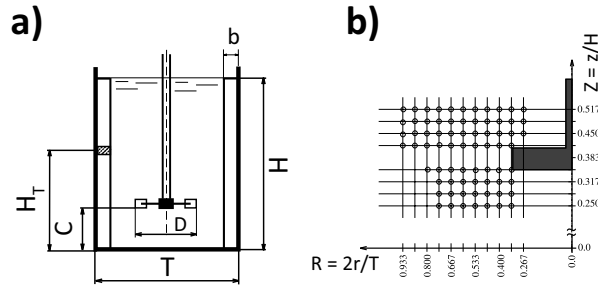
Fig. 1. a) Stirred tank configuration, b) measuring points in the stirrer region. Dimensions: $T = 0.29\,\mathrm{m}$, $H = T$, $D = 0.333\,T$, $b = 0.1\,T$. C is adjustable impeller off-bottom clearance, H_T denotes vertical position of the mechanical measuring target.

liquids. Three values of the impeller Reynolds number, Re_M,

$$Re_M = \frac{\varrho\, N D^2}{\eta},\qquad(1)$$

have been attained: 750, 1 200 and 75 000. The flow regime in the tank therefore varied from strictly laminar to the highly turbulent one. In equation (1) D is the impeller diameter (m), N is impeller speed of rotation (s^{-1}) and ϱ and η are liquid density and viscosity (kg m^{-3}, Pa s), respectively. Details on the experiments can be found in Montes *et al.*[3] and Hasal *et al.*[8,9].

2.3   Force measurement

The tangential component of the force affecting the baffle was measured by a mechanical device described in detail by Kratěna *et al.*[6] and Hasal *et al.*[7]. The force was measured at several vertical distances, H_T/H, from the tank bottom (cf. Figure 1). At each target position the value of Re_M was varied over the entire accessible range. The study was performed using either pitched blade impellers (with six or four blades, pitch angle 45^0, pumping downwards) at two off-bottom clearances, $C/H = 0.2$ and 0.35, or the Rushton turbine impeller at the off-bottom clearances $C/H = 0.35$ and 0.5. Water and cold and hot aqueous glycerol solutions were used as working liquids. A range of the Re_M values from 16 000 to 83 300 was achieved with the PBTs. The attainable range of the Re_M values of the RT was 6 000 to 63 000.

3   Experimental data analysis

Raw measured signals were numerically re-sampled with the sampling period $T_S = 20$ ms. Resulting time series were used for subsequent analysis. Procedures used for data analysis are mentioned here only briefly as the details can

a)   b)
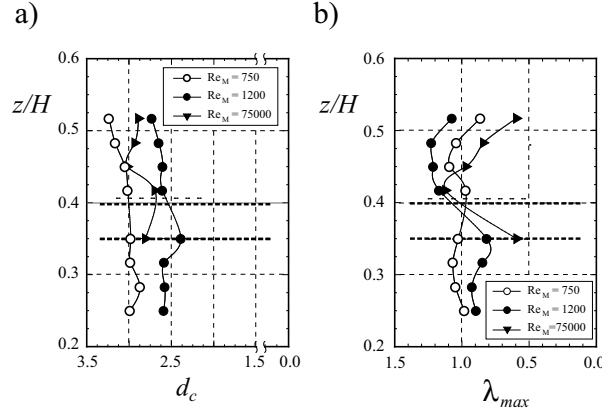
Fig. 2. Vertical profiles of a) averaged correlation dimension, d_c, and b) averaged maximum Lyapunov exponent, λ_{max}, of chaotic attractors of macro-instability component of axial component of liquid velocity at three impeller Reynolds number values. The d_c and λ_{max} values were obtained by averaging across individual horizontal levels of measuring points (cf. figure 1b). z denotes vertical coordinate. Heavy dashed lines delimit impeller position.

be found elsewhere, see, e.g., Hasal et al.[7–9], Broomhead and King[13] and Aubry et al.[14]. Recently we have established a technique enabling to detect the macro-instability in measured time series, evaluate its relative magnitude and reconstruct its temporal evolution, Hasal et al.[7,8]:

First, the presence of the macro-instability in the data is detected and its frequency determined using power spectra of the time series (using a FFT-based algorithm, Press et al.[15]). The procedure used for extraction of the MI-related component of the signal consists in an application of the proper orthogonal decomposition (POD) – see, e.g., Aubry et al.[14] or Broomhead and King[13] – combined with the spectral analysis. The measured data is in this procedure decomposed to a set of the eigenmodes and eigenvalues. A value of the k-th eigenvalue expresses relative contribution of the k-th eigenmode to the total variance of the analysed signal. By (properly) summing the eigenmodes a time evolution of the macro-instability related component of the analysed data can be reconstructed. The eigenmodes contributing to the macro-instability are selected from the entire set using their power spectra (cf. Hasal et al.[7–9]). The chaotic attractors of the macro-instability related components of the measured data were reconstructed using either the POD eigenmodes or the method of delays. The embedding dimension was determined using the false nearest neighbour analysis. The time delay value was determined from position of first minimum of mutual information function. Values of maximum Lyapunov exponent was determined using the TISEAN package procedures, Hegger et al.[16].
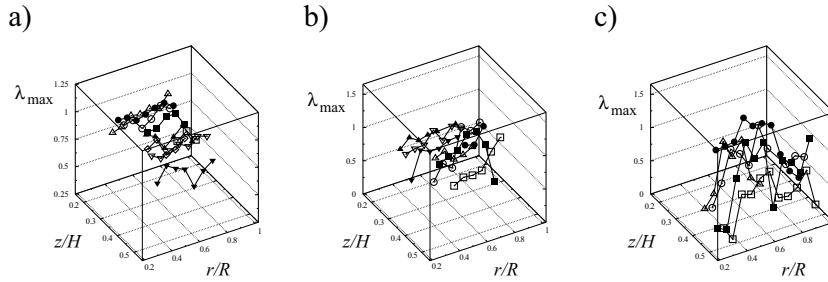
Fig. 3. Spatial distribution of maximum Lyapunov exponent, λ_{max}, of chaotic attractors of macro-instability component of axial liquid velocity at three impeller Reynolds number values: a) $Re_M = 750$, b) $Re_M = 1200$, c) $Re_M = 75\,000$. Different symbols are used only to distinguish horizontal levels of measuring points (cf. Figure 1).

4   Results and Discussion

We concentrated in our analyses predominantly to reconstruction of chaotic attractors of the macro-instability related components of measured fluid flow data and to evaluations of their chaotic invariants. We make use of the correlation dimension in order to characterize the temporal complexity of the MI flow component in a particular experimental point and further we evaluated maximum Lyapunov exponent value as it measures speed of divergence of trajectories in the phase space and therefore it may indicate a speed (magnitude) of dispersive processes produced by the macro-instability at given location within the tank.

Vertical profiles of correlation dimension and maximum Lyapunov exponent values for chaotic attractors of the MI component of the axial fluid velocity are shown in Figure 2. The plots in the Figure show values of both invariants averaged across horizontal levels of experimental points (cf. Figure 1) in order to suppress fluctuations of individual values. The correlation dimension value (Figure 2a) shows only minor variability with vertical position in the vessel. The effect of the impeller rotational speed is much more pronounced. The dynamics of temporal evolution of the MI component of fluid velocity is therefore almost coherent over the entire experimental region. The vertical profiles of the maximum Lyapunov exponent value (Figure 2b) shows more variability. The effect of the impeller speed is again obvious but also remarkable differences between λ_{max} values in the above impeller region and in the below impeller region are evident. This difference arises from different structure and properties of fluid streams in these two regions, cf., e.g., Kresta and Wood[1]. Figures 3 and 4 give more detailed views of the spatial distributions of the λ_{max} and d_c values over the mesh of the experimental points.
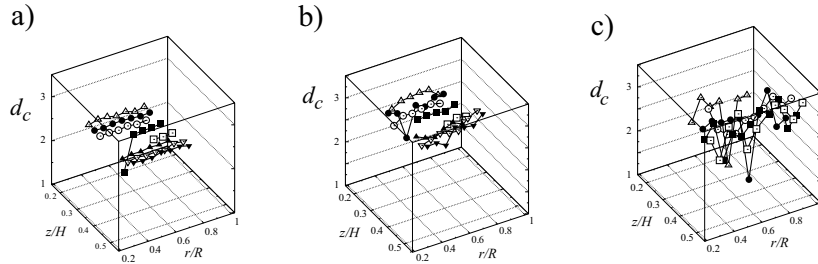
Fig. 4. Spatial distribution of correlation dimension, d_c, of chaotic attractors of macro-instability component of axial liquid velocity at three impeller Reynolds number values: a) $Re_M = 750$, b) $Re_M = 1200$, c) $Re_M = 75\,000$. Different symbols are used only to distinguish horizontal levels of measuring points (cf. figure 1).

The distributions of λ_{max} values in Figure 3 obviously reflects principal influence of the Reynolds number (Re_M) value on macro-instability dynamics: at very high intensity of mixing ($Re_M = 75\,000$, Figure 3c) the macro-instability flow component is destroyed (to a remarkable extent) by the stochastic turbulent flows. The extraction of the MI component of fluid velocity is less reliable at these points and so is also the evaluation of chaotic invariants of its attractors (considerable scatter of points in Figure 3c). The λ_{max} distributions are more homogeneous at lower Re_M values, cf. plots in Figures 3a,b. Higher values of the maximum Lyapunov exponent in the above impeller subregion of measuring points is evident. When mixing tank is designed for a dispersive process the inlet ports or pipes would be introduced just into this above impeller region.

The correlation dimension, d_c, exhibits quite homogeneous radial distributions (Figure 4), i.e., its values do not change much with the r/R value (except of the scattered distribution evaluated at $Re_M = 75\,000$). The dependence of the d_c values on vertical position, z/H, is more pronounced. The above and below impeller regions clearly differ in d_c value. Structures of state spaces of dynamical systems generating the MI flows below and above impeller regions are therefore different and reflects well known different structures of liquid flows in these regions.

The vertical distributions of the maximum Lyapunov exponent of attractors of the MI component of the tangential force affecting the radial baffle are shown in Figure 5 for three different impellers at the same off-bottom clearance, $C/H = 0.35$, and at various impeller speeds. The plots in Figure 5 – despite of the scatter of the points – reflect the basic structure of the fluid flows in mixing tanks equipped with the impellers used in our experiments. The PBTs induce single-loop circulation patterns with only relatively small differences between the above impeller and the below impeller parts of the liquid batch in the tank. As a consequence, the plots in Figures 5a,b ex-
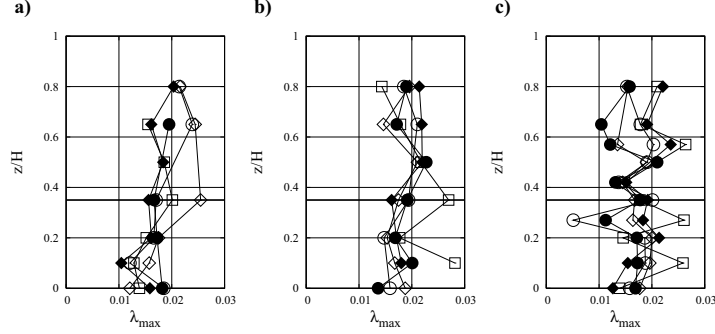
Fig. 5. Vertical distribution of maximum Lyapunov exponent, λ_{max}, of chaotic attractors of tangential force affecting the baffle. a) 6 bladed pitched blade impeller, b) 4 bladed pitched blade impeller, c) Rushton turbine impeller. Cold glycerol solution used as working liquid in all cases, impeller off-bottom clearance $C/H = 0.35$. Impeller speed of rotation: $\circ$...360 min^{-1}, $\bullet$...400 min^{-1}, $\Diamond$...440 min^{-1}, $\blacklozenge$ ...480 min^{-1}, $\square$ ...520 min^{-1} for PBTs; $\circ$...200 min^{-1}, $\bullet$...240 min^{-1}, $\Diamond$...280 min^{-1}, $\blacklozenge$ ...320 min^{-1}, $\square$ ...360 min^{-1} for RT impeller.

hibit relatively low vertical variability, the only exception can be the below impeller region with the 6PBT impeller (Figure 5a) where the λ_{max} takes markedly lower values. Here the impeller discharge stream (probably) destroys the macro-instability flow. Contrary, the Rushton turbine impeller evoked two-loop circulation pattern in the tank, where several vertically distributed regions can be identified differing in the direction of flows and in the turbulence intensity. The graphs in Figure 5c roughly reflect this flow structure. The effects of the impeller rotation frequency are also obvious – higher impeller speeds lower the λ_{max} values as the MI component of the flow becomes more destroyed by the turbulence.

5 Conclusions

The analyses performed in this work clearly demonstrated chaotic nature of the macro-instability of the flow pattern in mixing tanks used in experiments. Despite certain scatter of maximum Lyapunov exponent and correlation dimension values numerically determined for attractors of the extracted macro-instability components of the measured data regions with distinct dynamical behaviours can be detected within the vessel. The correlation dimension of the MI attractor is suitable for analysis of transitions between different flow patterns in the tank and of different MI types resulting from these transitions. The maximum Lyapunov exponent (taking distinctly positive values) can be used for finding regions with different MI dynamics within the tank and thus for finding proper location of inlet and outlet ports of continuous flow mixers, location of gas spargers or analytical probes etc.

References

1. S.M. Kresta and P.M. Wood. The mean flow field produced by a 45° pitched blade turbine: changes in the circulation pattern due to off-bottom clearance. *Canad. J. Chem. Eng.* 71:42-53, 1993.

2. O. Brůha, I. Fořt, P. Smolka and M. Jahoda. Experimental study of turbulent macro-instabilities in an agitated system with axial high-speed impeller and with radial baffles. *Collect. Czech. Chem. Commun.* 61:856-867, 1996.

3. J.-L. Montes, H.-C. Boisson, I. Fořt, and M. Jahoda. Velocity field macro-instabilities in an axially agitated mixing vessel. *Chem. Eng. J.* 67:139-145, 1997.

4. L. Nikiforaki, G. Montante, K.C. Lee and M. Yianneskis. On the origin, frequency and magnitude of macro-instabilities of the flows in stirred vessels. *Chem. Eng. Sci.* 58:2937-2949, 2000.

5. K.J. Bittorf and S.M. Kresta. Active volume of mean circulation for stirred tanks agitated with axial impellers. *Chem. Eng. Sci.* 55:1325-1335, 2000.

6. J. Kratěna, I. Fořt, O. Brůha and J. Pavel. Distribution of dynamic pressure along a radial baffle in an agitated system with standard Rushton turbine impeller. *Trans. I.Chem.E.* 79A:819-823, 2001.

7. P. Hasal, I. Fořt and J. Kratěna. Force effects of the macro-instability of flow pattern on radial baffles in a stirred vessel with pitched-blade and Rushton turbine impellers. *Chem. Eng. Res. Des.* 82A:1268-1281, 2004.

8. P. Hasal, J.-L. Montes, H.-C. Boisson and I. Fořt. Macro-instabilities of velocity field in stirred vessel, detection and analysis. *Chem. Eng. Sci.* 55:391-401, 2000.

9. P. Hasal, and I. Fořt. Macro-instabilities of the flow pattern in a stirred vessel: Detection and characterization using local velocity data. *Acta Polytechnica* 40:55-67, 2000.

10. J.M. Ottino, F.J. Muzzio, M. Tjahjadi, J.G. Franjione, S.C. Jana and H.A. Kusch. Chaos, symmetry, and self-similarity: Exploiting order and disorder in mixing processes. *Science* 257:754-760, 1992.

11. C. Letellier, L. Le Sceller, G. Gousbet, F. Lusseyran, A. Kemoun and B. Izrar. Recovering deterministic behavior from experimental time series in mixing reactor. *AIChE J.* 43:2194-2202, 1997.

12. N. Matsuda, Y. Tada, S. Hiraoka, S. Qian, H. Takeda, K. Ishida and Y. Mouri. Frequency components related to the macro-instabilities of flow in an agitated vessel. *Kagaku Kogaku Ronbunshu* 29:327-332, 2003.

13. D.S. Broomhead and G.P. King. Extracting qualitative dynamics from experimental data. *Physica* 20D:217-236, 1986.

14. N. Aubry, R. Guyonnet and R. Lima. Spatiotemporal analysis of complex signals: Theory and applications. *J. Stat. Phys.* 64:683-739, 1991.

15. W.H. Press, S.A. Teukolsky, W.T. Vetterling and B.P. Flannery. *Numerical Recipes in FORTRAN.* Cambridge: Cambridge University Press 1992.

16. R. Hegger, H. Kantz and T. Schreiber. Practical implementation of nonlinear time series methods: The TISEAN package. *CHAOS* 9:413-435, 1999.